JOURNAL OF GEOPHYSICAL RESEARCH, VOL. 115, A00E41, doi:10.1029/2009JA014834, 2010

Click Here for Full Article

Free-running ground-based photometric array imaging of transient luminous events

R. T. Newsome[1] and U. S. Inan[1,2]

Received 25 August 2009; revised 29 October 2009; accepted 1 March 2010; published 7 July 2010.

[1] We present observations of transient luminous events (TLEs) recorded during a summer TLE observation campaign in 2008 at Langmuir Laboratory near Socorro, New Mexico. The campaign featured observations made by a free-running, ground-based multianode photometric array called the Photometric Imager of Precipitated Electron Radiation (PIPER). As a photometric array, PIPER has high (40 μs) temporal resolution and enough spatial resolution (16 anodes per photometer) to make it particularly useful in the study of fast TLEs like elves and halos. As a free-running instrument, there are no missed detections and no unwanted sampling bias introduced by triggering. As a ground-based instrument, it can follow individual storms over the course of their lifetime rather than randomly sampling over large numbers of storms as required by space-based instruments. During the campaign, 143 sprites, 803 elves, and 166 halos were observed over six storms, resulting in averaged elve-to-sprite and halo-to-sprite occurrence ratios of 5.6:1 and 1.2:1, respectively. There was considerable variability in the elve-to-sprite occurrence ratio from storm to storm, ranging from a low of 3.7:1 to a high of 13.4:1. Overall, 78.2% of the elves and 55.4% of the halos were associated with negative cloud-to-ground lightning strikes (−CGs); no sprites associated with −CGs were observed. Additionally, 40 events in which pairs of elves occur in rapid succession, events we refer to as elve doublets, were observed in several storms. The duration between elves in the elve doublet events was typically 120 μs. The causative mechanism for these events is still under deliberation.

Citation: Newsome, R. T., and U. S. Inan (2010), Free-running ground-based photometric array imaging of transient luminous events, *J. Geophys. Res.*, *115*, A00E41, doi:10.1029/2009JA014834.

1. Introduction

[2] In the past two decades, researchers studying the upper atmosphere and lower ionosphere have discovered a menagerie of brief, optical flashes resulting from thunderstorm lightning, collectively referred to as transient luminous events (TLEs). These optical phenomena include elves, halos, and sprites. Elves are a particularly transient (<1 ms in duration) class of TLE that occur as rapidly expanding luminous rings at ionospheric *D* region altitudes (~90 km) [*Inan et al.*, 1997] and are the optical signature of ionospheric electron heating resulting from the electromagnetic pulse (EMP) radiated by lightning return stroke currents [*Inan et al.*, 1991, 1997]. Halos are similarly brief (<2 ms), diffuse optical emissions at mesospheric altitudes around 70 km, due to heating produced by quasi-electrostatic (QE) fields set up by the rearrangement of the thunderstorm cloud charge configuration affected by a cloud-to-ground (CG) lightning stroke [*Pasko et al.*, 1997; *Barrington-Leigh et al.*, 2001]. Sprites consist of highly structured, rapidly moving, and longer-lasting (>10 ms) streamers propagating to lower mesospheric and upper stratospheric altitudes (down to 40 km), initiated by the same QE fields that produce halos [*Pasko et al.*, 1997]. While halos and sprites share similarities (versus elves) as far as causative mechanisms are concerned, halos and elves share morphological similarities (spatially simple structure on similar 1 ms time scales) not shared by sprites.

[3] Since the first published TLE observation in 1989 [*Franz et al.*, 1990], elves, halos, and sprites have been observed optically in a variety of ways. Early observations concentrated on sprites (and their associated halos) and involved ground-, aircraft-, and space shuttle–based intensified video-rate and high-speed cameras [e.g., *Lyons*, 1994; *Sentman et al.*, 1995; *Boeck et al.*, 1995]. The first elve observation was made from a space shuttle intensified video-rate camera [*Boeck et al.*, 1992], and the first ground-based optical observations of elves were made by Fukunishi using three vertically arranged photometers [*Fukunishi et al.*, 1996]. Subsequent ground-based observations of elves have typically been made with video-rate cameras and/or triggered photometric arrays [*Inan et al.*, 1997;

[1]Space, Telecommunications, and Radioscience Laboratory, Stanford University, Stanford, California, USA.
[2]Koç University, Istanbul, Turkey.

Copyright 2010 by the American Geophysical Union.
0148-0227/10/2009JA014834

Barrington-Leigh and Inan, 1999; *Miyasato et al.*, 2002]. In 2007, the Imager of Sprites and Upper Atmospheric Lightning (ISUAL) team completed a three year satellite-based TLE observation campaign that included an autonomously triggered high-speed camera and photometric array that observed elves, halos, and sprites in large numbers [*Chen et al.*, 2008]. This study concluded, surprisingly at the time, that elves were easily the most common class of TLE (roughly 9 elves observed for each observed sprite) and, among other things, that elves and halos occur over water and coastal areas at almost twice their overland rates. These satellite-based TLE observations represent globally averaged TLE production rates.

[4] In this paper, we present results from a ground-based TLE observation campaign using a free-running photometric array instrument called the Photometric Imager of Precipitated Electron Radiation (PIPER). As a photometric instrument, PIPER has high temporal resolution making it particularly useful in the study of elves and halos. As a photometric array, it has enough spatial resolution to discriminate elves from halos, but not so much spatial resolution that triggering mechanisms are required. As a free-running instrument, there are no missed detections and no unwanted sampling bias introduced by the act of triggering (which is normally required in high-speed imaging applications due to the large amount of data generated per acquisition). As a ground-based instrument, it can follow the TLE production of a single storm over its lifetime (rather than randomly sampling over large numbers of storms as required by space-based instruments). The chief advantage of such an instrument is in the ability to study fast TLEs on a per-storm (rather than individual or global) basis. We concentrate specifically on observations of elves and halos.

2. Instrumentation

[5] During July and early August 2008, Stanford conducted a TLE observation campaign at Langmuir Laboratory, near Socorro, New Mexico. The instrumentation included a photometric array instrument called PIPER [*Marshall et al.*, 2008], an unintensified wide-field-of-view video-rate camera, and a two-component magnetic loop ELF/VLF antenna and receiver [*Cohen et al.*, 2010]. During the postcampaign data analysis, we also used lightning stroke location and peak current data from the National Lightning Detection Network (NLDN).

2.1. PIPER

[6] PIPER is a photometric array imager designed and built at Stanford University for electron precipitation and TLE observations. It makes use of two Hamamatsu photometer arrays turned at right angles to each other. As the 16 anodes of each array are laid out in a line, one array gives the vertical distribution of light in the field of view while the other gives the horizontal distribution of light in the field of view. The photometer anodes are sampled at 25000 samples/s, allowing for 40 μs time resolution, and each has an 18° by 1.125° rectangular field of view (resulting in a total field of view that is an 18° square).

[7] The basic principal behind PIPER, as far as TLE observation is concerned, is that trading spatial resolution for time resolution permits observation of TLEs that are otherwise difficult to image with more traditional cameras. PIPER's 40 μs time resolution is sufficient for the observation of brief TLEs like elves and halos (both of which last less than 2 ms). Its small number of spatial elements (the photometer anodes) permit discrimination between TLEs of distinct geometries (elves and halos) and prevents the data acquisition rate from being so high that a triggering mechanism is required. Thus, PIPER can run continuously in a free-running mode for hours on end and the data can be processed afterward. This improves detection rates, as there are no missed detections due to failure to trigger or downtime during rearming of the trigger.

[8] The recorded data is processed by finding, automatically, all the times in which the field of view brightened suddenly. This is accomplished by averaging all the anodes of the vertical photometer together to create one 25000 sample/s time series and then breaking the time series into 1 ms segments. For each 1 ms segment, the segment's sample mean and sample standard deviation is computed. The first 10 segments of a data record are labeled "typical" and each subsequent segment is compared to the last 10 typical segments: if the segment's sample mean is more than 1 standard deviation greater than the average segment mean of the last 10 typical segments, the segment is labeled "interesting"; otherwise, it is labeled "typical". After all the interesting segments are automatically identified, the full PIPER data corresponding to each interesting segment is examined by hand to determine if the segment contained a TLE (and what kind) or not.

2.2. Video-Rate Camera

[9] An unintensified Watec WAT-902H3 Ultimate camera was mounted on top of PIPER such that its field of view was coaligned with that of the PIPER photometers. The video-rate camera field of view is 32° wide and 22° tall and completely contains the PIPER field of view. The camera CCD is a black and white CCD and is most sensitive in the optical range of wavelengths, which of course includes the N_2 first positive (1P) and N_2^+ first negative (1N) emissions of sprites.

[10] The video-rate camera is used primarily to find TLEs (especially sprites) in real time during each night of the campaign so that both the camera and PIPER can be pointed accurately. Of the 165 halos and 40 elve doublets observed, only 16 (9.7%) of the halos and none (0%) of the elve doublets were observed in the video-rate camera. The detection rate of these <2 ms events is much higher (around 10 times higher) in PIPER than it is in the video-rate camera.

2.3. AWESOME VLF Receiver

[11] An AWESOME ELF/VLF receiver and antenna was set up at Langmuir Laboratory to record the VLF sferics launched by the CGs causing the TLEs observed by PIPER and our video-rate camera. The receiver setup consists of two orthogonal air-core loop antennas to measure both horizontal components of the local magnetic field. The receiver is sensitive from ~800 Hz to 47 kHz and exhibits a linear phase response over this range of frequencies. Due to efficient sferic propagation in the Earth-ionopshere wave-

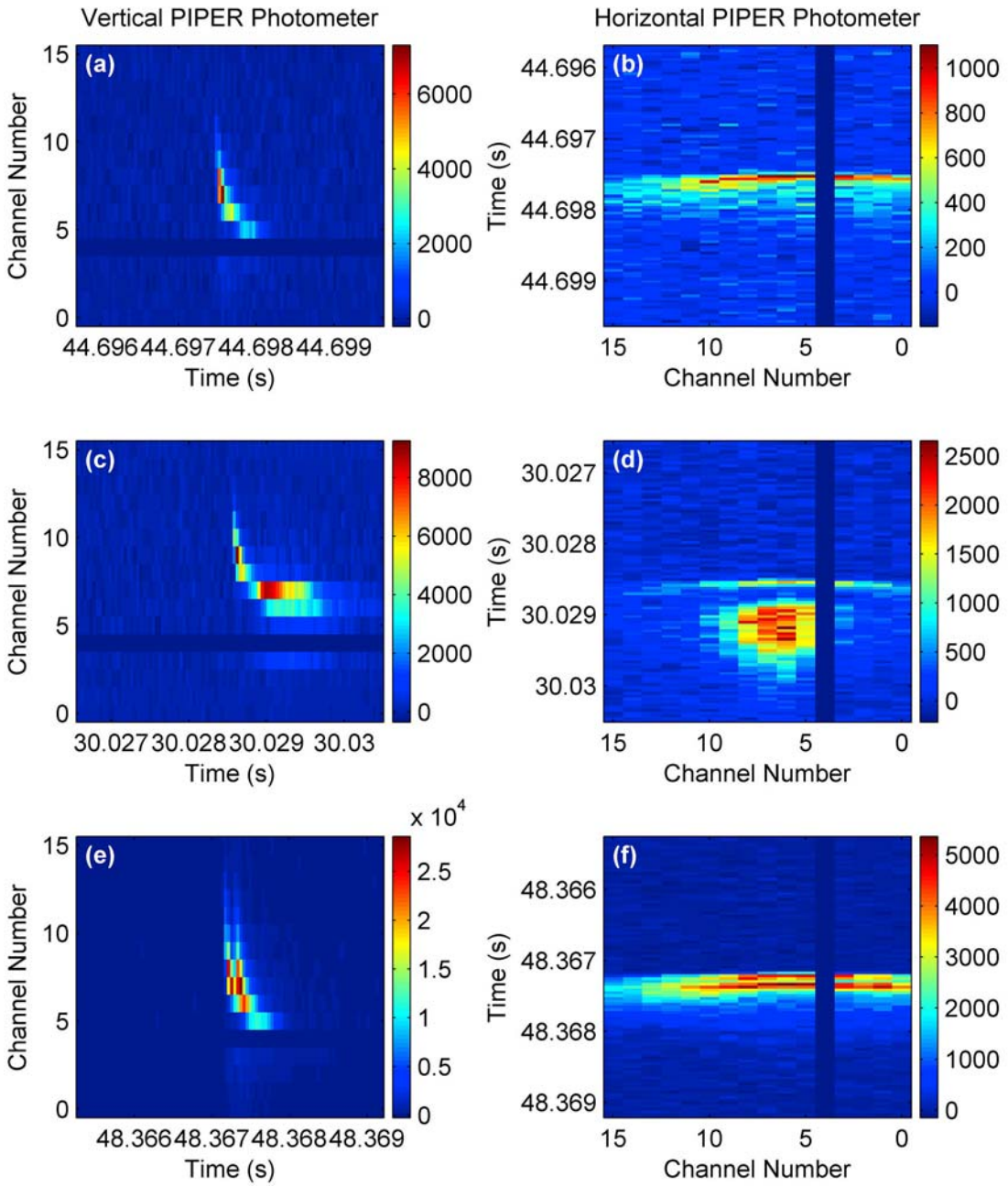


Figure 1. Examples of TLEs as observed by PIPER. (left) Vertical photometer data (showing the vertical distribution of light in the field of view as time progresses from left to right) and (right) horizontal photometer data (showing the horizontal distribution of light in the field of view as time progresses from top to bottom). The intensities are plotted on separate arbitrary linear scales. (a and b) The first example is an elve, (c and d) the second example is an elve and a halo, and (e and f) the third example is an elve doublet. Note that anode 4 of each photometer is a bad anode due to a wiring fault and should be ignored.

guide, the receiver is easily sensitive enough to detect incoming sferics originating from locations well beyond the ~1000 km range for optical detection by PIPER. The received magnetic field waveforms are digitized (with a sampling rate of 100 kHz) and recorded locally with GPS-synchronized time stamping. A more expanded discussion of the technical details of the AWESOME ELF/VLF receiver is given by *Cohen et al.* [2010].

3. Observations

[12] Figures 1a and 1b show an example of an elve as seen by PIPER. Figure 1a shows the vertical distribution of light

Table 1. TLE Counts by Storm During a Summer TLE Observation Campaign Conducted From Langmuir Laboratory in 2008[a]

	Sprites			Elves			Elve + Halos			Elve Doublets		
Storm (Date)	Events	+CG	−CG	Events	+CG	−CG	Events	+CG	−CG	Events	+CG	−CG
1 (24 July)	42	100%	0%	157	33.1%	66.9%	42	52.4%	47.6%	2	0%	100%
2 (28 July)	0	-	-	2	50%	50%	0	-	-	0	-	-
3 (29 July)	28	100%	0%	285	18.9%	81.1%	42	54.8%	45.2%	10	0%	100%
4 (30 July)	5	100%	0%	67	10.4%	89.6%	5	40%	60%	14	0%	100%
5 (1 Aug)	1	100%	0%	6	16.7%	83.3%	0	-	-	0	-	-
6 (2 Aug)	67	100%	0%	286	21.0%	79.0%	77	35.1%	64.9%	14	0%	100%
All	143	100%	0%	803	21.8%	78.2%	166	44.6%	55.4%	40	0%	100%

[a]Campaign totals and distributions of causative CG polarity (as determined from VLF recordings) are also reported. Note that the sets of elve + halo and elve doublets events are subsets of the set of elve events and are, with the exception of one event, themselves disjoint.

from the vertical photometer as time evolves from left to right. Figure 1b shows the horizontal distribution of light from the horizontal photometer as time evolves from top to bottom. In array photometry such as PIPER, elves appear as down-and-to-the-right curves in a vertical array and as flattened horizontal arcs in a horizontal array. The form of these curves is due to the fact that the first photons to arrive at the instrument are emitted from the portion of the elve closest to the instrument (i.e., at higher elevation angles and in the center of the field of view) and subsequent photons are emitted from the portions of the elve further away (i.e., at lower elevation angles and on the edges of the field of view) [*Barrington-Leigh et al.*, 2001]. Note that anode 4 of both the vertical and horizontal photometers are bad anodes and can be ignored: these two anodes' signals were carried off the PIPER instrument by a shared signal cable that was found afterward to have been slightly damaged; the other anode signals did not share the damaged cable.

[13] Figures 1c and 1d show an example of an elve and a halo as observed by PIPER. The halo is an emission lasting between 0.3 ms and 2 ms, and appears in the PIPER data toward the bottom of the elve in the vertical photometer (i.e., behind the elve's approaching edge) and centered underneath the elve in the horizontal photometer (presumably above the causative CG). Elves and halos are easily distinguishable in photometer array data due to the high temporal resolution. In video-rate camera data, where the temporal resolution is lower, elves and halos are less easy to distinguish and more easily confused.

[14] While array photometry discriminates between elves and halos more easily than video-rate camera data, it does not discriminate between halos and sprites as easily as video-rate camera data (due to the low spatial resolution of the array as compared to the high spatial resolution of the camera CCD). In PIPER data, sprites look similar to halos. The most distinguishable difference is the duration of the emission: sprites can last for several to tens of ms, whereas halos last less than 2 ms.

[15] Through the course of the 2008 TLE observation campaign, a number of observations were made of what appears to be pairs of elves occurring in very rapid (less than 500 μs) succession of each other. In this paper, we refer to these events as elve doublets. Figures 1e and 1f show an example of an elve doublet in PIPER data. An earlier example of an elve doublet was also reported by *Barrington-Leigh and Inan* [1999, Figure 2]. We investigate these events in more detail below.

[16] In the 2008 TLE observation campaign, six storms were observed between July 24 and August 2. Three of these storms (July 24, July 29, and August 2) were large storms that produced large numbers of TLEs. One of these storms (July 30) was a medium-sized storm, and the remaining two storms were very small. (The terms "large", "medium", and "small" here are used quite loosely: suffice it to say that all the "large" storms averaged more than 30 elves/hour for at least 4 hours or more after sundown, all the "small" storms averaged less than 5 elves/hour and lasted no longer than 2 hours after sundown, and the one "medium" storm was somewhere in between.) Table 1 summarizes the numbers of each class of TLE observed on a per-storm basis. From received VLF sferics, we determined the polarity of the causative CG associated with each PIPER-observed TLE; Table 1 thus also shows the breakdown of causative CG polarity by TLE class on a per-storm basis, as well as totals for the entire campaign. Note that in Table 1, the counts of elve + halos and elve doublets are subsets of the counts of elves. That is, an elve + halo/elve doublet event is counted both in the elve + halo/elve doublet column as well as in the elve column. As discussed later, with the exception of one event, there were no examples of elve doublets associated with halos; the sets

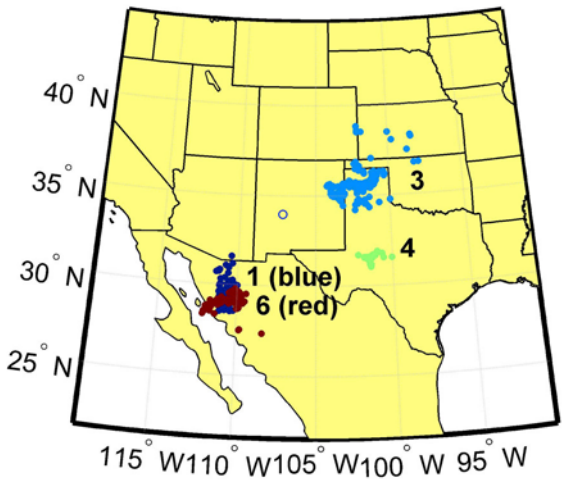


Figure 2. Map of NLDN-reported elve-producing CGs by storm during 2008. The labeled storm numbers correspond to those in Table 1. The location of Langmuir Lab is denoted by the open circle.

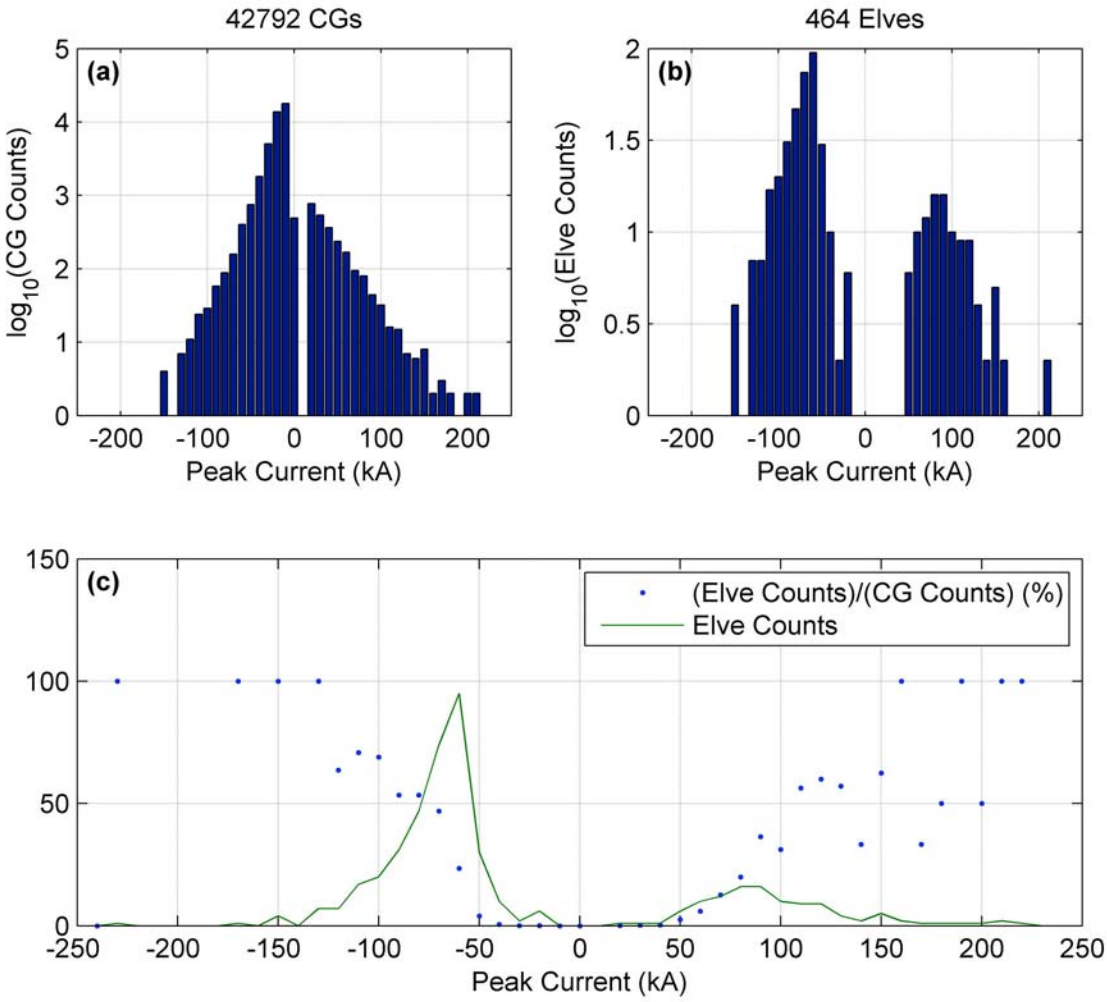


Figure 3. Histograms of NLDN-identified peak currents (a) for CGs and (b) for CGs that produced PIPER-identified elves. (c) The ratio of elve-producing CG counts to total CG counts (expressed as a percent, blue dots), giving an idea empirically of how often a CG of a particular peak current produced an elve. The elve-producing CG counts are also plotted (green line) to give an idea of how statistically significant the sample of each peak current bin is.

of elve + halos and elve doublets in Table 1 are nearly disjoint. Figure 2 shows the geographic distribution of the elve observations for the four largest storms in Table 1.

4. Discussion

4.1. Elves

[17] Overall, we see from Table 1 that 143 sprites, 803 elves, and 166 halos were observed to accompany a total of 1112 CG strikes. This suggests an average elve-to-sprite occurrence ratio of 5.6:1, somewhat lower than the three year globally averaged ratio of 8.6:1 reported by *Chen et al.* [2008, Table 2]. Considering only the overland observations of *Chen et al.* [2008], however, it far exceeds the globally averaged overland ratio of 1.6:1. The difference in the two rates (our rate and the globally averaged overland rate of *Chen et al.* [2008]) results from the fact that a ground-based instrument can commit all its observation time to known-to-be-active thunderstorms whereas satellite-based instruments only get to observe storms for which the storm trajectory and satellite orbit coincidentally overlap. That these two rates vary so greatly suggests that elve production over land is highly concentrated in large thunderstorms, as one might expect.

[18] It is worth pointing out that there is a pronounced variability in TLE occurrence ratios from storm to storm. For the four largest storms (storms 1, 3, 4, and 6), the elve-to-sprite ratio ranged from as low as 3.7:1 (storm 1) to as high as 13.4:1 (storm 4).

[19] With regard to causative CG polarity, most elves are caused by −CGs. This is not surprising, as elve production should depend primarily on the strength of a CG's radiated EMP and not on CG polarity. There are far more −CGs than +CGs and, while +CGs may tend to be more intense (higher peak currents) than −CGs, one would still expect more elves to be actually due to −CGs than +CGs. It is likely that most of the variability in elve-causing CG polarity (e.g., compare storm 1 to storm 4) is due to variability in the overall number of +CG and −CG strikes in a storm with which an elve can be produced.

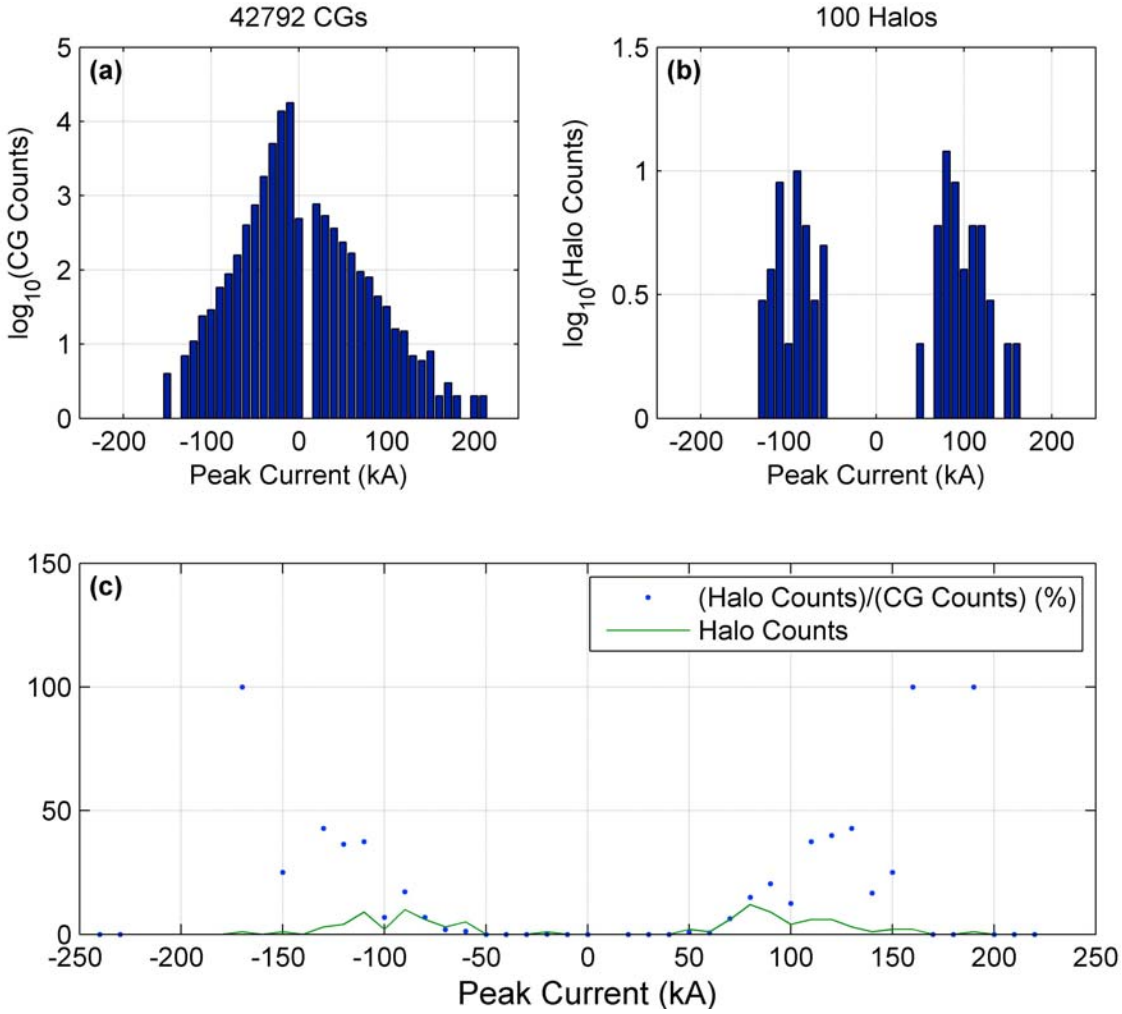


Figure 4. Histograms of NLDN-identified peak currents (a) for CGs and (b) for CGs that produced PIPER-identified halos. (c) The ratio of halo-producing CG counts to total CG counts (expressed as a percent, blue dots), giving an idea empirically of how often a CG of a particular peak current produced a halo. The halo-producing CG counts are also plotted (green line) to give an idea of how statistically significant the sample of each peak current bin is.

[20] A subset (around 60%) of the total observed VLF sferics could be associated in retrospect with CG detections reported by NLDN, which also provides useful information including CG location and peak current. (The seemingly low NLDN detection rate of 60% is due largely to the fact that a large number of our elve observations were made of storms in northern Mexico, just outside NLDN's primary coverage region.) In making assignments of NLDN reports to PIPER elve events, we considered only NLDN reports of CGs occurring <4 ms before the elve and within 15° in azimuth of the center of PIPER's field of view at the event's time of occurrence. If we restrict our attention to only those sferics (and whatever TLEs they may have caused), we can plot histograms of the CG peak currents (Figure 3a) and of the elve-producing CG peak currents (Figure 3b).

[21] We note that the empirical peak current distribution of all CGs follows those reported elsewhere [*Rakov and Uman*, 2003, p. 146], with the following typical trends: most CGs are negative and have a peak current magnitude less than 50 kA, while most CGs with peak current magnitudes exceeding 100 kA are positive. For the elve-producing CGs, most are negative with peak current magnitudes less than 100 kA (probably reflecting the fact that there are simply not many large −CGs with which to produce an elve to begin with). There are many elve-producing +CGs as well, but most have peak current magnitudes exceeding 50 kA.

[22] Figure 3c shows the ratio (as a percentage, see the blue dots) of elve-producing CG counts to total CG counts for each peak current bin. This result is an estimate of the probability of a CG of a given polarity and peak current to produce an elve. The total number of elve-producing CGs is reproduced (green line) on the same axis to remind the reader that estimates for the extreme peak current CGs are based on very few observations and should be viewed with more suspicion.

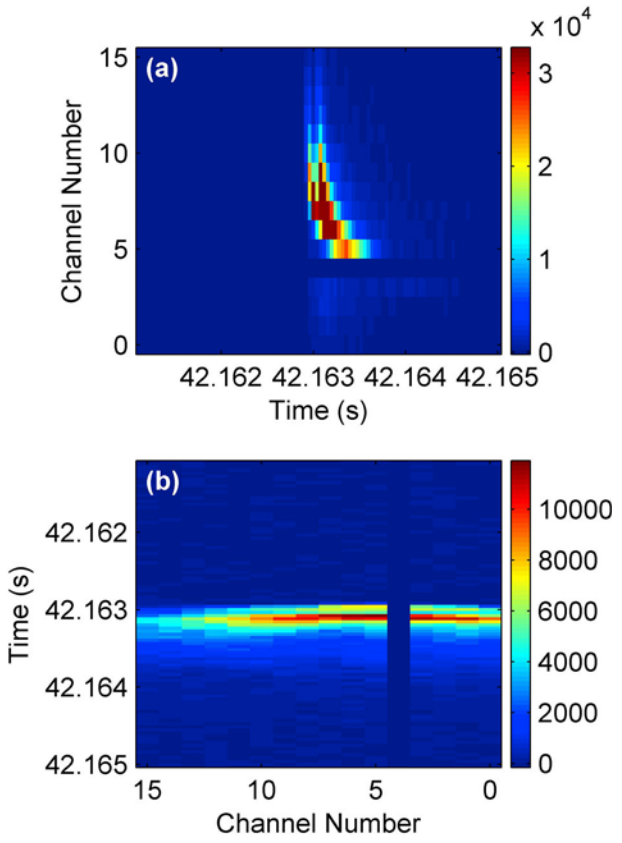


Figure 5. Another example of an elve doublet as observed by PIPER. (a) Vertical photometer data, showing the vertical distribution of light in the field of view as time progresses from left to right. (b) Horizontal photometer data, showing the horizontal distribution of light in the field of view as time progresses from top to bottom. The intensities are plotted on separate arbitrary linear scales. Note again that anode 4 of each photometer is a bad anode due to a wiring fault and should be ignored.

[23] We see that although Figure 3b suggests a small number of relatively small (<50 kA) elve-producing CGs, these events make up an insignificant fraction of the total number of small CGs. We also see what appears to be a sort of threshold for producing elves in the peak current: CGs with peak current magnitudes exceeding 50 kA produced elves a nonnegligible fraction of the time during this observation campaign. This result suggests that the CG peak current magnitude may be a useful proxy for estimating the strength of the CG's radiated EMP, as previously discussed by *Kuo et al.* [2007].

4.2. Halos

[24] Referring back to Table 1, our observed average halo-to-sprite occurrence ratio is 1.2:1. The globally averaged ratio from *Chen et al.* [2008, Table 2] is 1.0:1, and the globally averaged overland ratio is 0.4:1. Again, these differences are likely a result of our ground-based instrument's ability to watch strictly active thunderstorms while satellite-based instruments can only watch regions over which their orbit takes them. From storm to storm, the halo-to-sprite ratio varied less than the elve-to-sprite ratio did, ranging from as low as 1.0:1 (storms 1 and 4) to as high as 1.5:1 (storm 3).

[25] For halos, +CGs and −CGs were involved in nearly even numbers. This is in contrast to reports of overwater halos by *Frey et al.* [2007], where nearly all events were associated with −CGs, and of overland halos by *Bering et al.* [2004], where over 60% of events observed in 2 storms were associated with +CGs.

[26] Figure 4 repeats the contents of Figure 3 for the case of halo-producing CGs. Figure 4a is identical to Figure 3a. In Figure 4b, we see that halos are associated in roughly equal numbers with larger CGs (peak current magnitudes greater than 50 kA) of both polarities. Figure 4c suggests again a peak current magnitude threshold for halo production of around 50 kA for both +CGs and −CGs, and suggests no real preference in polarity for halo production.

4.3. Elve Doublets

[27] Elve doublets, events in which pairs of elves seem to appear in rapid succession, were observed in the 4 largest storms (storms 1, 3, 4, and 6). An example of an elve doublet as recorded in PIPER data was shown in Figure 1; another example is shown in Figure 5.

[28] Figure 6 shows the distribution of elve counts for each of these storms. For the three largest storms (storms 1, 3, and 6), the lone elves, elve + halos, and elve doublets

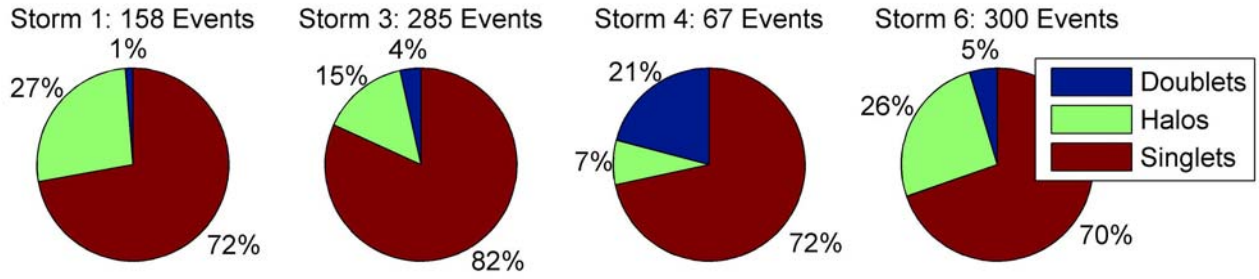


Figure 6. Distributions of counts of observed elves on a per-storm basis for four different storms. "Doublets" refers to elve doublet events, "Halos" refers to elve + halo events, and "Singlets" refers to observations of elves not accompanied by secondary elves (as in elve doublet events) or halos (as in elve + halo events). Note that these three categories, with the exception of only one elve doublet accompanied by a halo, are strictly non-overlapping.

Table 2. Elve Separations in Time for Elve Doublet Events

Separation (μs)	Count
<60	0
60–100	6
100–140	24
140–180	10
>180	0

appeared in roughly the same proportions, with elve doublets making up no more than 5% of the total elve count. In the one medium-sized storm (storm 4 on July 30), a much larger percentage of the elves were elve doublets. Referring to Table 1, this storm produced few sprites (only 5, compared to ~30+ for the other storms) and was likely not the same meteorological class of storm as the larger storms 1, 3, and 6. Of all the elve observations, there was only one instance of an elve doublet accompanied by a halo.

[29] A total of 40 elve doublets were observed over 4 storms. The mean separation in time between the elves over these 40 events was 124 μs, although PIPER's 40 μs time resolution makes precise measurement of this value difficult. Table 2 summarizes the observations.

[30] Figure 7a shows VLF sferics recorded for elve events, including elve doublet events, from the July 29 storm (storm 3) all plotted on the same axis. The green traces are sferics associated with 265 of the non-doublet elves, while the blue traces are sferics associated with all 9

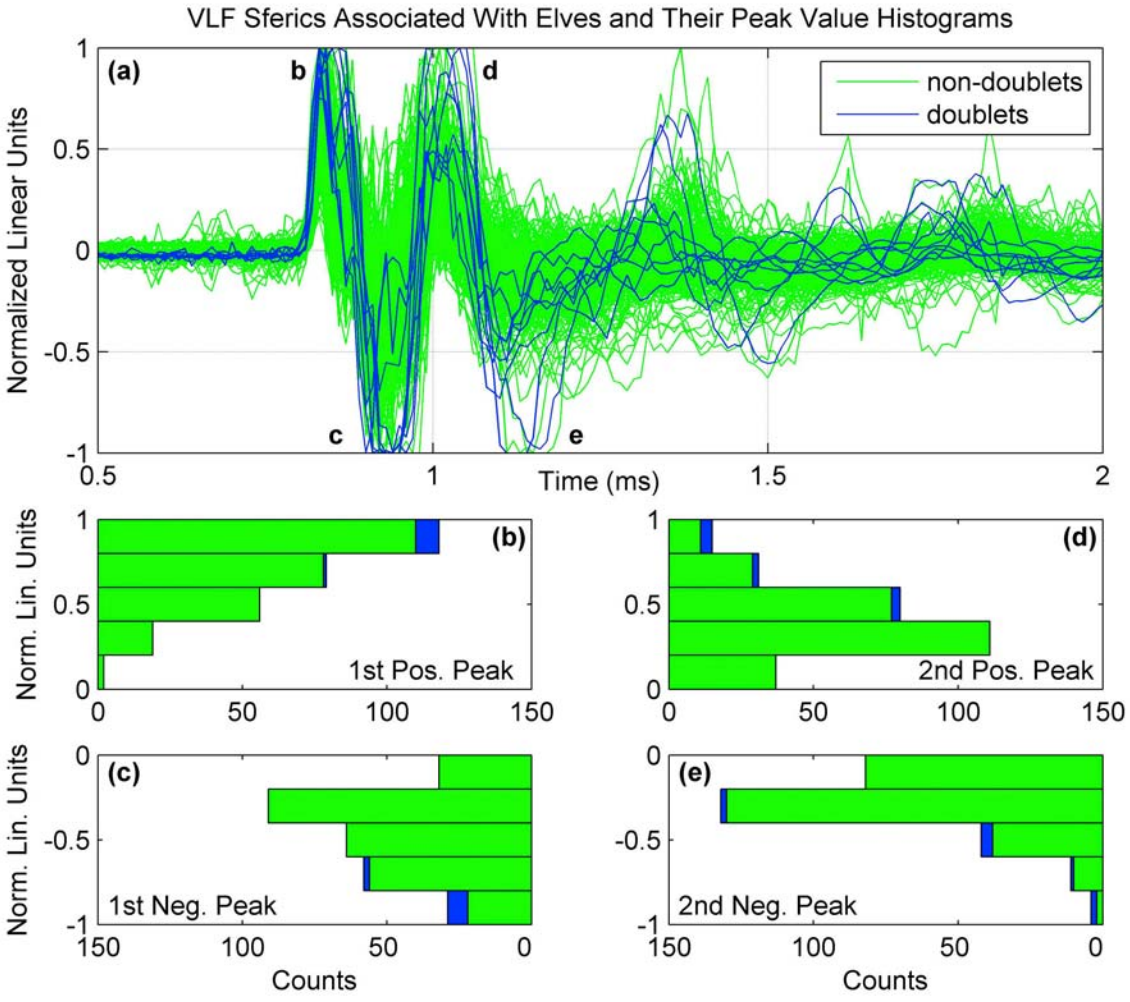


Figure 7. (a) VLF sferics from the July 29 storm, plotted on the same axis. The green traces are 265 sferics associated with non-doublet elves, and the blue traces are all 9 sferics associated with doublet elves. The amplitude axis is in normalized linear units, where −1 and +1 represent the maximum measurable magnetic field of the AWESOME VLF receiver. (b–e) Histograms of the peak VLF values for the first four sferic peaks: the first positive peak (Figure 7b), the first negative peak (Figure 7c), the second positive peak (Figure 7d), and the second negative peak (Figure 7e). The green regions of the histograms represent counts of non-doublet-associated sferics, while the blue regions represent counts of doublet-associated sferics. Note that the count axes in Figures 7c and 7e are reversed for effect: the zero-count locations of the four histograms occur right-to-left in the order in which the peaks occur in the sferic (first positive, first negative, second positive, and then second negative).

of the elve doublets. Figures 7b–7e are histograms of the peak VLF values for the first four sferic peaks: the first positive peak (Figure 7b), the first negative peak (Figure 7c), the second positive peak (Figure 7d), and the second negative peak (Figure 7e). The green regions of Figures 7b–7e represent counts of non-doublet-associated sferics, while the blue regions represent counts of doublet-associated sferics.

[31] It is clear from Figure 7 that sferics associated with elve doublet events are intense (in magnitude) and exhibit multiple strong initial peaks. While there were also a few examples of non-doublet sferics that are intense with multiple strong initial peaks, most are less intense in magnitude and have at most one strong initial peak. Consider the sferics' peak value histograms of Figures 7b–7e. For the first positive peak (Figure 7b), all sferics' peak values tend to be large regardless of whether they are associated with elve doublet values or not. For the first negative peak (Figure 7c), more non-doublet-associated sferics have lower peak values while all the doublet-associated sferics remain large. This trend continues for the second positive peak (Figure 7d) and, to a more limited degree, even the second negative peak (Figure 7e).

[32] We can rule out a few candidate causative mechanisms for these elve doublet events. They are likely not caused by multiple return strokes spaced closely in time, as it is unlikely that a second strong return stroke would consistently occur 120 μs after the initial return stroke (the typical interstroke period being 60 ms [*Rakov and Uman*, 2003, p. 8]). It is also not likely that the second optical emission is due to a ground reflection of the radiated EMP reaching the ionosphere at a slightly later time. The 120 μs delay represents an additional optical path length of 36 km (assuming free space propagation), which would require the EMP source to be located 18 km above the ground, too high for a CG or even intercloud/intracloud lightning.

[33] That the received VLF sferic also exhibits a doubly peaked nature suggests that the cause lies in the return stroke waveform itself. Without access to the actual return stroke waveform, it is difficult to see exactly what happened. Most likely, the radiated EMP of the return stroke simply exhibits multiple peaks (perhaps from the ramping up and then ramping down of current) which cause multiple elves. Further investigation is necessary.

5. Summary

[34] We presented photometric array observations of transient luminous events recorded during a summer TLE observation campaign conducted in July and early August 2008 at Langmuir Laboratory near Socorro, New Mexico. The observation campaign featured a free-running, ground-based array photometry instrument called PIPER as well as a video-rate camera and a VLF antenna and receiver. The PIPER instrument is capable of following a single storm from the ground for hours without missed detections due to triggering issues. It has high temporal resolution and adequate spatial resolution, making it ideal for observing particularly fast TLEs like elves and halos. PIPER observed many TLEs, including large numbers of sprites, elves, halos, and elve doublets. Most elves were caused by −CGs with smaller (<75 kA) peak currents, while CGs with >50 kA peak currents began to have a significant empirical probability of producing elves. Halos observed by PIPER were associated with both −CGs and +CGs in roughly equal numbers. A large number of elve doublets, events in which pairs of elves appeared in rapid succession, occurred over 4 different storms. The separation between the elves in these events was typically 120 μs, and the causative mechanism is still under deliberation.

[35] **Acknowledgments.** This work was supported in part by a Texas Instruments Stanford Graduate Fellowship and by ONR grant N00014-03-1-0333 to Stanford University. The PIPER instrument was built under support from the High-frequency Active Auroral Research Program (HAARP), the Air Force Research Laboratory (AFRL), the Defense Advanced Research Programs Agency (DARPA), and the Office of Naval Research (ONR) via ONR grants N00014-00-1-0643, N00014-05-C-0308, and N00014-03-100630 to Stanford University. We thank William P. Wynn of New Mexico Tech for hosting us at Langmuir Laboratory, and we thank NLDN for providing the lightning location data used during the observation campaign and in subsequent data analysis.

[36] Zuyin Pu thanks the reviewers for their assistance in evaluating this paper.

References

Barrington-Leigh, C. P., and U. S. Inan (1999), Elves triggered by positive and negative lightning discharges, *Geophys. Res. Lett.*, *26*, 683–686.

Barrington-Leigh, C. P., U. S. Inan, and M. Stanley (2001), Identification of sprites and elves with intensified video and broadband array photometry, *J. Geophys. Res.*, *106*, 1741–1750.

Boeck, W. L., O. H. Vaughan Jr., R. Blakeslee, B. Vonnegut, and M. Brook (1992), Lightning induced brightening in the airglow layer, *Geophys. Res. Lett.*, *19*, 99–102.

Boeck, W. L., O. H. Vaughan Jr., R. J. Blakeslee, B. Vonnegut, M. Brook, and J. McKune (1995), Observations of lightning in the stratosphere, *J. Geophys. Res.*, *100*, 1465–1475.

Bering, E. A., III, J. R. Benbrook, L. Bhusal, J. A. Garrett, A. M. Paredes, E. M. Wescott, D. R. Moudry, D. D. Sentman, H. C. Stenbaek-Nielson, and W. A. Lyons (2004), Observations of transient luminous events (TLEs) associated with negative cloud to ground (−CG) lightning strokes, *Geophys. Res. Lett.*, *31*, L05104, doi:10.1029/2003GL018659.

Cohen, M. B., U. S. Inan, and E. W. Paschal (2010), Sensitive broadband ELF/VLF radio reception with the AWESOME instrument, *IEEE Trans. Geosci. Remote Sens.*, *48*, 3–17.

Chen, A. B., et al. (2008), Global distributions and occurrence rates of transient luminous events, *J. Geophys. Res.*, *113*, A08306, doi:10.1029/2008JA013101.

Franz, R. C., R. J. Nemzek, and J. R. Winckler (1990), Television image of a large upward electrical discharge above a thunderstorm system, *Science*, *249*, 48–51.

Frey, H. U., et al. (2007), Halos generated by negative cloud-to-ground lightning, *Geophys. Res. Lett.*, *34*, L18801, doi:10.1029/2007GL030908.

Fukunishi, H., Y. Takahashi, M. Kubota, K. Sakanoi, U. S. Inan, and W. A. Lyons (1996), Elves: Lightning-induced transient luminous events in the lower ionosphere, *Geophys. Res. Lett.*, *23*, 2157–2160.

Inan, U. S., T. F. Bell, and J. V. Rodriguez (1991), Heating and ionoization of the lower ionosphere by lightning, *Geophys. Res. Lett.*, *18*, 705–708.

Inan, U. S., C. Barrington-Leigh, S. Hansen, V. S. Glukhov, and T. F. Bell (1997), Rapid lateral expansion of optical luminosity in lightning-induced ionospheric flashes known as 'elves,' *Geophys. Res. Lett.*, *24*, 583–586.

Kuo, C.-L., et al. (2007), Modeling elves observed by FORMOSAT-2 satellite, *J. Geophys. Res.*, *113*, A11312, doi:10.1029/2007JA012407.

Lyons, W. A. (1994), Characteristics of luminous structures in the stratosphere above thunderstorms as imaged by low-light video, *Geophys. Res. Lett.*, *21*, 875–878.

Marshall, R. A., R. T. Newsome, and U. S. Inan (2008), Fast photometric imaging using orthogonal linear arrays, *IEEE Trans. Geosci. Remote Sens.*, *46*(11), 3885–5893.

Miyasato, R., M. J. Taylor, H. Fukunishi, and H. C. Stenbaek-Nielsen (2002), Statistical characteristics of sprite halo events using coincident photometric and imaging data, *Geophys. Res. Lett.*, *29*(21), 2033, doi:10.1029/2001GL014480.

Pasko, V. P., U. S. Inan, T. F. Bell, and Y. N. Taranenko (1997), Sprites produced by quasi-electrostatic heating and inonization in the lower ionosphere, *J. Geophys. Res.*, *102*, 4529–4561.

Rakov, V. A. and M. A. Uman (2003), *Lightning: Physics and Effects*, Cambridge Univ. Press, Cambridge, U. K.

Sentman, D. D., E. M. Wescott, D. L. Osborne, D. L. Hampton, and M. J. Heavner (1995), Preliminary results from the Sprites94 aircraft campaign: 1. Red sprites, *Geophys. Res. Lett.*, *22*, 1205–1208.

U. S. Inan and R. T. Newsome, Space, Telecommunications, and Radioscience Laboratory, Stanford University, Stanford, CA 94305, USA. (rtnewsome@stanford.edu)